Available online at www.sciencedirect.com
SCIENCE DIRECT®
Journal of Sound and Vibration 283 (2005) 201–215
JOURNAL OF SOUND AND VIBRATION
www.elsevier.com/locate/jsvi

Nonlinear dynamics of above-ground thin-walled tanks under fluctuating pressures

Eduardo M. Sosa, Luis A. Godoy*

Department of Civil Engineering and Surveying, University of Puerto Rico at Mayagüez, Mayagüez Campus, Mayagüez, Puerto Rico, PR 00681-9041, USA

Received 8 May 2003; accepted 6 April 2004
Available online 2 December 2004

Abstract

The nonlinear dynamics and stability of an empty above-ground steel tank is analyzed. The tank considered is one of the typical configurations found in the Caribbean Islands and in the United States, constructed with a cylindrical shell with variable thickness, and a conical roof supported by rafters. An assumed space variation of pressures and a simplified deterministic model of time fluctuating pressures due to wind are applied. The response is calculated by a finite element model of the tank using explicit integration of the equations of motion for several pressure levels and period of fluctuations. The dynamic buckling load is evaluated using the criterion due to Budiansky and Roth. The response is analyzed in the time and in the frequency domain in order to recognize the nature of the problem. The results show that pressure fluctuations do not induce resonance of the structure, so that simpler pressure models may be used in practical analysis.

1. Introduction

This paper investigates the nonlinear dynamic behavior and buckling of thin-walled steel tanks with a fixed conical roof, under a deterministic simulation of wind pressures. Above-ground storage tanks used in the oil and petrochemical industries are complex structures, frequently built

*Corresponding author. Tel.: +1-787-265-3815; fax: +1-787-833-8260.
E-mail address: lgodoy@uprm.edu (L.A. Godoy).

0022-460X/$ - see front matter © 2004 Published by Elsevier Ltd.
doi:10.1016/j.jsv.2004.04.023

with a cylindrical body, a roof (either fixed or floating in the vertical direction), and an additional structure to support the roof [1]. Typical designs of short tanks make use of very thin shells, with relations between the radius of the cylinder and the wall thickness of the order of 1500–2000, and height to diameter ratios of less than 0.5. Because of the slenderness of the shell, buckling has been reported under high winds or hurricanes [2–4] and is a major constraint in the design.

Most studies reported in the technical literature of buckling of tanks under wind are restricted to open tanks. In addition, the results consider a static analysis of the problem and disregard the possibility of any dynamic effect due to wind [4,6–11]. However, wind gusts induce transient vibrations in the shell during short times, which may eventually lead to dynamic buckling.

In the design of tanks in the United States, wind gusts of 3 s duration at 10 m above ground surface are considered, with wind velocities of 64 m/s in the Eastern Coast and the Caribbean islands [5]. Preliminary results using wind pressures in the form of a rectangular impulse with 3 s duration seem to indicate that the dynamic effects are not significant in terms of the buckling capacity of the shell. However, the question remains if pressure fluctuations within a 3 s impulse may have a more damaging effect on the stability of the shell, and thus justify an empirical investigation of such fluctuations in wind records. This paper addresses this question by means of a nonlinear dynamic analysis of a specific tank with a conical roof.

The outline of the paper is as follows: the model of fluctuating pressure adopted in this work is described in Section 2. Such a pressure model is applied to a theme structure described in Section 3. Section 4 deals with the dynamic response of the structure in the time domain, and in Section 5 the analysis is carried out in the frequency domain. Finally, conclusions are presented in Section 6.

2. Wind action

Typical wind records measure wind velocity every 3 s; however, no information is obtained for intervals of less than 3 s, so that any fluctuations in the velocity (and in the consequent pressures on the structure) are eliminated from the data. Such information is not relevant for most types of structures, but for thin-walled tanks, it may be important in order to understand the nature of buckling. From the information provided by wind records, it seems that an adequate load configuration would be an impulsive pressure with 3 s duration. The only studies reported in the literature including wind as an impulsive pressure on tanks consider a constant pressure during 3 s, or else a step variation [2,3].

At present, there are no extensive records regarding the values or the nature of pressure fluctuations for periods less than 3 s, and the question remains open if it is necessary to obtain such data because it may have a significant influence on the behavior of a tank structure. To investigate the influence of such fluctuations on the dynamic response of the shell one can resort to computer simulations. This paper reports studies using geometrically nonlinear dynamic analysis under impulsive loads with fluctuations in the pressure. The pressure fluctuations within a gust considered in this paper are shown in Fig. 1. There are two parameters involved in the definition of such pressures: first, there is a pressure fluctuation amplitude, P_f, and second, there is a fluctuation period, T_f. Non-dimensional quantities may be written as $\tau = T_f/T_3$ and $\eta = P_f/P_3$, where $T_3 = 3$ s and P_3 is the average value of the wind gust pressure.

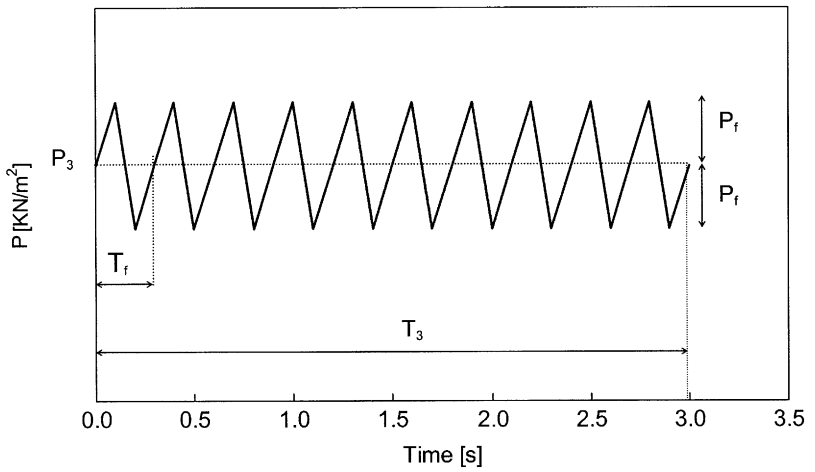

Fig. 1. Model of pressure variation with time. Rectangular impulse with fluctuations. T_f, period of the fluctuation; T_3, 3 s interval; P_f, fluctuation amplitude of the; P_3, average amplitude pressure.

To carry out the computations, a pressure distribution reported by MacDonald et al. [12], which was obtained from wind-tunnel experiments, has been adopted. Fig. 2(a) shows contours of the pressures used on the roof and Fig. 2(b) gives the pressure distribution used on the cylindrical wall. The present model assumes that the pressures are applied simultaneously on the complete surface of the structure. Of course, there are many uncertainties regarding the pressure distribution, and at present, this is an open topic for research. It is not clear how several factors influence the wind pressures in real tanks, such as topographic effects, roughness of the terrain, interaction with other tanks, and others. The present investigation considers pressures on an isolated tank in an open terrain. A more refined model should include the change in pressures as wind moves on the surface of the shell; however, this refinement is outside the scope of the present investigation.

3. Representative structure and computational model

The tank investigated in this paper is representative of typical tanks found in the United States, and the geometry and dimensions are shown in Fig. 3(a). The same geometry has been employed by the authors for the analysis of static buckling due to support settlement [13].

The tank is modeled by means of a finite element discretization using a general-purpose finite element program [14]. Approximately 12,000 quadrilateral and triangular linear shell elements are used to model both the cylindrical shell with a tapered wall and the conical roof. Additionally, the rafters that support the conical shell are included in the model; they have the shape and dimensions found in usual real tanks. Specifically in this research, a W8 × 13 steel section according to AISC code was used to model the rafters. The rafters were modeled with quadrilateral linear shell elements and placed in a radial configuration supporting the conical roof as shown in Fig. 3(b). The tank is assumed to be fixed at the base and has additional boundary conditions at the top of the conical roof to simulate the presence of a central column by means of

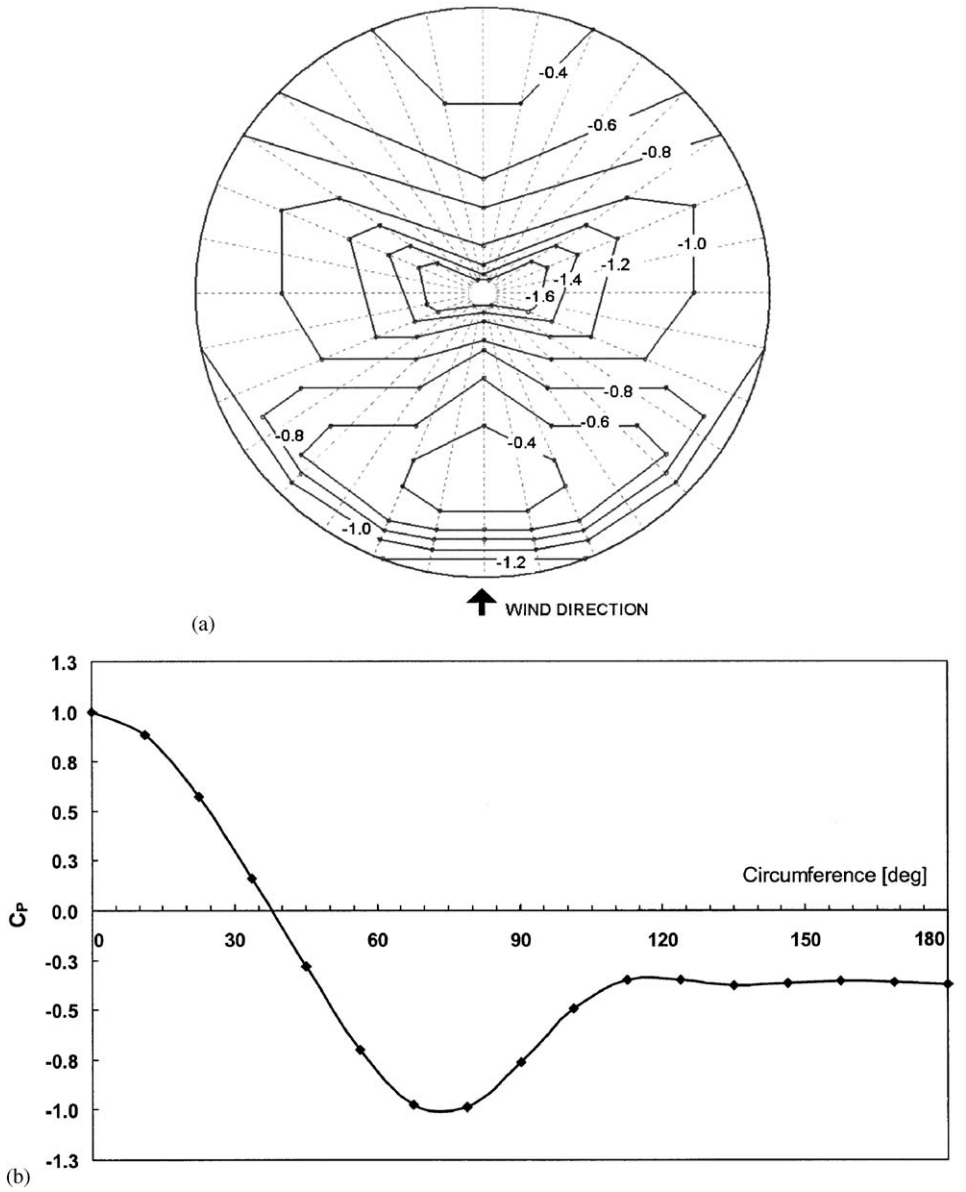

Fig. 2. Contours of wind pressures used in computations: (a) pressure distribution on the conical roof; (b) pressure distribution on the cylindrical shell.

constraints in the vertical displacements of the rafters, but allowing free translations in the horizontal plane and free rotations. The junction between the cylindrical wall and the conical roof is continuous.

Geometrical nonlinear dynamics analyses have been carried out to evaluate the response of the tank to spatial and temporal variations of the pressure. For this kind of analysis, explicit integration of the equation of motion is performed. The analysis calculates the response at time

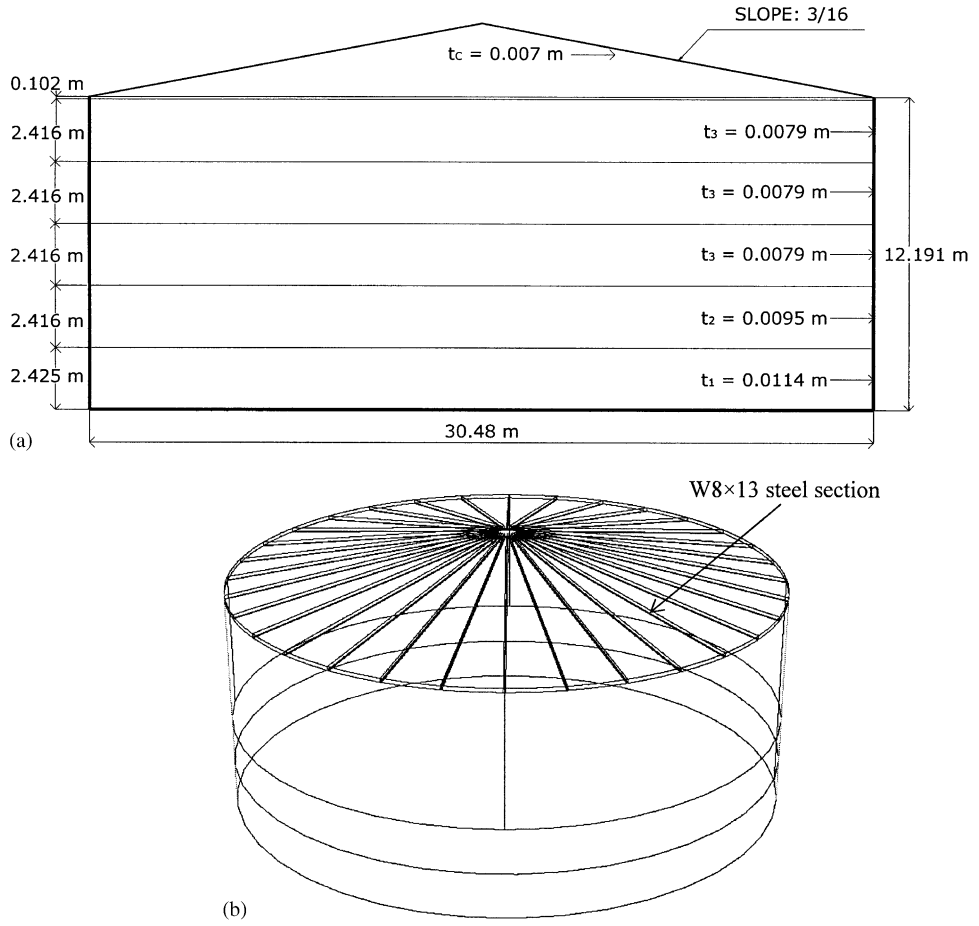

Fig. 3. Details of the tank considered in the analyses: (a) dimensions; (b) overview of conical shell and configuration of the rafters.

$[t+\Delta t]$ using the values at time $[t]$. Very small time increments are necessary to make the algorithm stable. The constitutive material is elastic, with modulus of elasticity $E=2.06\mathrm{E}+08\,\mathrm{kN/m^2}$, Poisson's ratio $v=0.3$, and density $\rho=7800\,\mathrm{kg/m^3}$. Material damping has been considered in parametric studies.

4. Nonlinear dynamic response

The dynamic buckling criterion employed in this work is due to Budiansky and Roth [15]. This is a qualitative criterion and requires the computation of the transient geometrically nonlinear response of the shell for different levels of dynamic pressures. The main variables involved in the criterion are the dynamic pressure and a displacement (or a displacement component). Dynamic buckling occurs if, for a small increment in the load, there is a large increment (at least one order of magnitude) in the transient displacements at a given time. In other words, dynamic buckling

occurs at the lowest pressure level that produces a fast transition from small to large transient displacements. This criterion requires expensive computations, i.e. the geometrically nonlinear transient response of a system with many degrees of freedom, and many trials are necessary to find the dynamic buckling load. Other publications have adopted this criterion for the evaluation of a dynamic buckling load in tanks (see for example Refs. [2,3] and those cited there).

First, let us consider a pressure distribution without any fluctuation, and with a 3 s time of application of the load. The space distribution of pressures is shown in Fig. 2, with contour values in kN/m^2, and to increase the values of pressures at all points, a non-dimensional scalar parameter λ is used. The pressure configuration in Fig. 2 is for $\lambda = 1$. The relation between velocity and pressure is that given by ASCE-7-02 [5]. Fig. 4(a) shows the nonlinear dynamic response computed numerically. For $\lambda = 2.50$ and 2.51 the oscillations have small amplitude and would vanish in the presence of material damping. The lowest value of λ for which divergent oscillations are computed is for $\lambda = 2.515$ (or wind velocity of about 64.4 m/s), in which case there are small amplitude oscillations up to a time $t = 2.16$ s, and then the amplitude increases by two orders of magnitude (increasing from 7 to 150 mm). As the load is increased, i.e. $\lambda = 2.52$ or $\lambda = 2.60$, the structure becomes unstable at earlier times. According to the criterion of Budiansky and Roth, the dynamic buckling load is $\lambda_D = 2.515$ and finding this value involves a sequence of computations for different load levels. The deflected shape of the shell, as it becomes unstable at the load λ_D, is shown in Fig. 4(b) at the onset of instability ($t = 2.16$ s), and at an advanced buckled state ($t = 3$ s) in Fig. 4(c). The practical significance of the wind velocities computed depends on the location of the tank, and these are not uncommon velocities in the Caribbean region and in the eastern coast of the United States where hurricane winds can reach considerable high values.

Second, to understand the influence of pressure fluctuations in time, let us consider the case with $\eta = 0.1$ and $\tau = 0.25$. The procedure to identify dynamic buckling is repeated and yields a value of $\lambda_D = 2.34$ (or wind velocity of about 61.3 m/s), that is, a smaller multiplier than in the first case. For a given value of η, the value of λ_D is seen to be dependent on τ, so that it becomes important to understand the relation between λ_D and τ.

The natural frequencies of the tank were computed with the same software [14] and are listed in Table 1. For the present case, the higher period (lower frequency) is $T_N = 0.3562$ s, which is smaller than the period of the excitation of both cases considered previously. Thus, a fluctuation having $T_f = T_N$ would be a bad situation for the structure, since there is coupling between the frequencies of the load and the structure. The results of transient displacements for $T_f = T_N$ are plotted in Fig. 5(a), and the dynamic buckling modes at the onset of the stability and for an advanced buckled state are given in Figs. 5(b) and (c), respectively. The dynamic buckling load results in $\lambda_D = 2.34$ (or wind velocity of about 61.8 m/s), which is smaller than the value obtained for the first pressure model but larger than the value for the second model.

A more complete picture of the problem may be obtained from a parametric study in which τ is changed and the transient response is computed. The results are plotted in Fig. 6 in terms of λ_D versus τ. First, it seems that the changes are not as drastic as one may imagine: the variations in λ_D are of the order of 10% with respect to the value for a rectangular pressure impulse. Second, the lowest values of λ_D are not necessarily associated to the lowest natural frequency of the shell. This is so because the pressure pattern applied to the shell yields deflections that are not coincident with the fundamental mode of vibration of the tank.

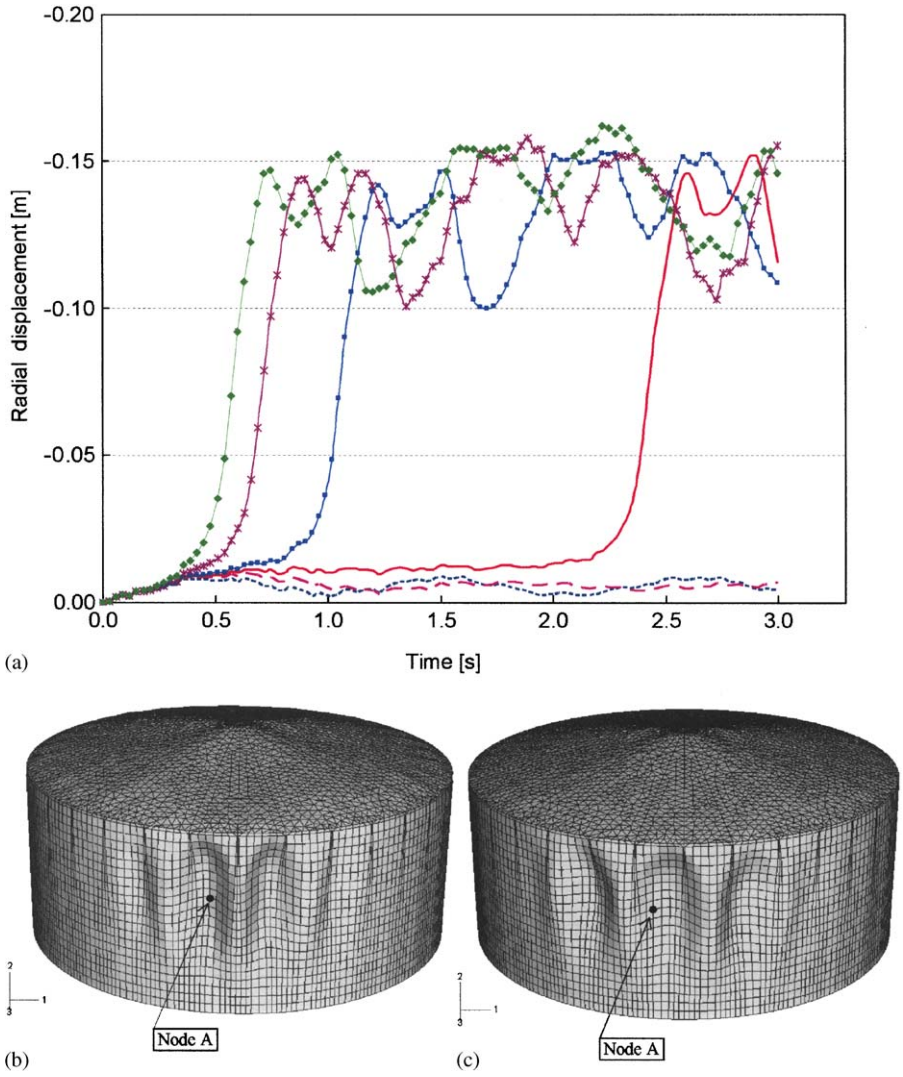

Fig. 4. Tank under constant impulsive load. (a) Displacement versus time for node A: - - - -, $\lambda = 2.50$; — —, $\lambda = 2.51$; —, $\lambda = 2.515$; —■—, $\lambda = 2.52$; — × —, λ=2.55; —◆—, $\lambda = 2.60$. (b) Buckling mode at the onset of instability; (c) deflected shape in an advanced buckled state.

All previous computations did not include damping, so it would be important to understand the influence of damping on the response. Typical steel tanks have a 3% damping ratio. Results were computed using Rayleigh damping, with a mass-proportional coefficient $\alpha_R = 1.848$ for a frequency in a cylinder mode of $\omega_{25} = 4.9036$ Hz. For the constant pressure in time reported in Fig. 4, the dynamic buckling load increased from 2.515 to 2.53, with a 0.6% increment. For the fluctuating pressure of Fig. 5, the influence of damping was to increase the dynamic buckling load from 2.34 to 2.36 (a 1.07% change). Because the influence is so small, it was decided to perform all the computations using zero damping.

Table 1
Natural frequencies of the shell

Mode	f (Hz)	T (s)	Mode	f (Hz)	T (s)	Mode	f (Hz)	T (s)
1	2.8077	0.3562	11	3.7563	0.2662	21	4.7698	0.2097
2	2.8134	0.3554	12	3.7784	0.2647	22	4.8082	0.208
3	2.9323	0.341	13	3.7801	0.2645	23	4.8694	0.2054
4	2.9349	0.3407	14	3.7853	0.2642	24	4.8974	0.2042
5	2.9642	0.3374	15	4.074	0.2455	25	4.9036	0.2039
6	2.9704	0.3367	16	4.107	0.2435	26	4.904	0.2039
7	3.1703	0.3154	17	4.3774	0.2284	27	4.9177	0.2033
8	3.1808	0.3144	18	4.416	0.2264	28	4.9191	0.2033
9	3.4571	0.2893	19	4.6372	0.2156	29	4.9591	0.2016
10	3.4661	0.2885	20	4.6706	0.2141	30	4.9638	0.2015

The imperfection sensitivity of buckling loads has not been addressed up to now; however, it is well known that imperfections play an important role in reducing the buckling load in static problems of tanks [4]. Small geometric imperfections, with amplitude of the order of the thickness of the shell, have been included in the analysis. The geometry of the imperfections was taken with the shape of the displacement pattern at the onset of dynamic buckling, which is significant only in the buckled region. For the imperfect shells, the nonlinear dynamic buckling studies under fluctuating pressures were repeated for the same parameters ($T_f = 0.356$, $\eta = 0.1$) used in Fig. 5, and a summary is presented in Fig. 7. The reduction in buckling load depends on the maximum amplitude of the imperfect shape, and for amplitude equal to the top shell thickness ($t_{\min} = 7.9$ mm), the reduction is about 30%. The shell, both under constant pressure in time and under fluctuating pressures, is equally affected by imperfections.

5. Frequency domain analysis

A frequency domain analysis of the perfect shell has been carried out for two time variations of the load: a rectangular impulse of 3 s and $\lambda = 2.515$; and a fluctuating pressure with $\lambda = 2.34$ and $T_f = 0.3562$ s (equivalent to an excitation frequency of 2.807 Hz, that is, the lowest natural frequency of the tank). The pressures chosen for the analysis are the lowest values for which the shell buckles before the 3 s period.

The shell response computed for the duration of 10 s is shown in Fig. 8 at the location of maximum radial displacements of the shell. For the rectangular impulse, the shell has large oscillations when the load is removed and the oscillations continue in the absence of damping. Under a fluctuating load, on the other hand, there are two clearly identified stages: small amplitude oscillations when the load is applied until buckling occurs and oscillations about the deflected shape once the load is removed.

The FFT for the complete history of displacements is shown in Fig. 9 (for a rectangular impulse) and in Fig. 10 (for fluctuating pressure). In the studies reported in this section, the cut-off frequency for $\Delta t = 0.03$ s is $f_c = 16.66$ Hz, so that a broad range of natural frequencies of the tank may be taken into account. The natural frequencies have been computed from an eigenvalue

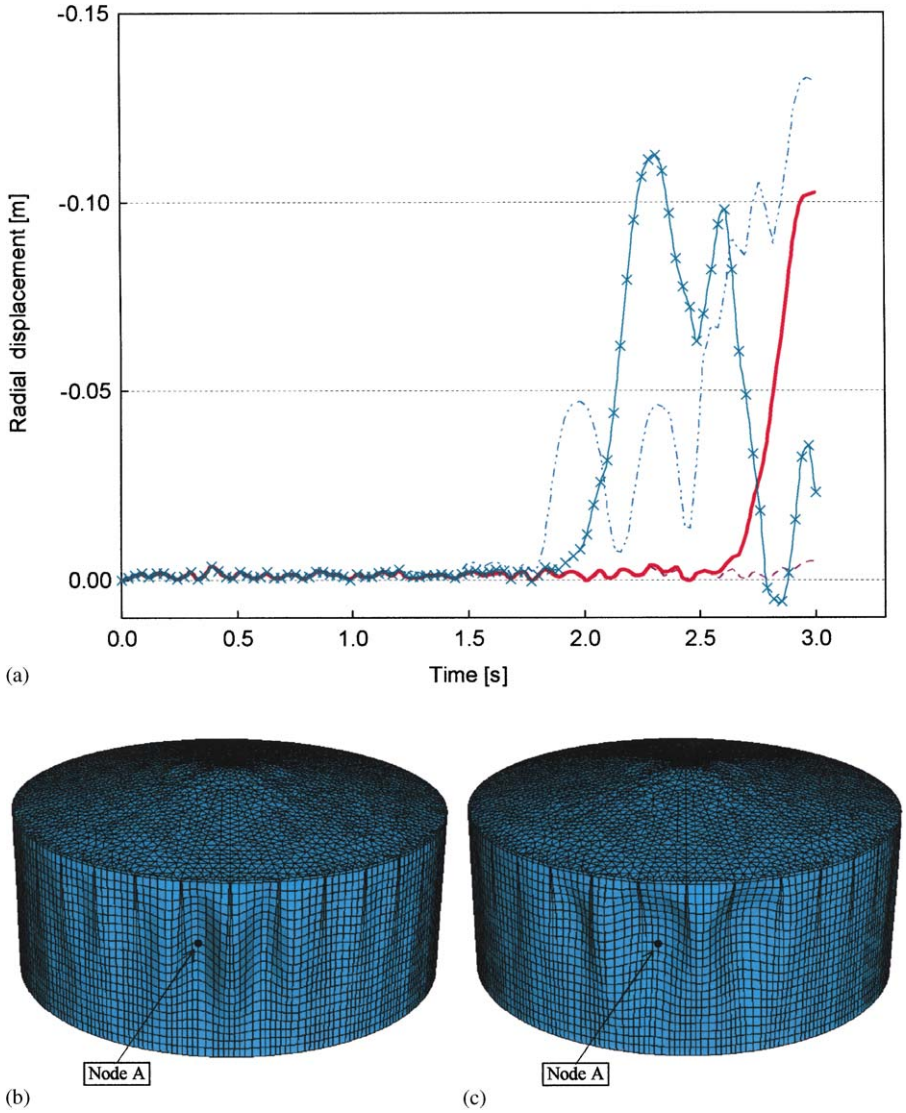

Fig. 5. Tank with impulsive load and fluctuation with $T_f = T_N$ and $\eta = 0.1$. (a) Displacement versus time for node A: – –, $\lambda = 2.335$; —, $\lambda = 2.34$; — × —, $\lambda = 2.55$; – · ·–, $\lambda = 2.60$. (b) Buckling mode at the onset of instability; (c) deflected shape in an advanced buckled state.

analysis and are included in Table 1. However, the results have been plotted up to a frequency of 5 Hz because for higher frequencies the amplitudes are negligible and do not provide additional information.

Figs. 9(a) and 10(a) show the FFT of the response, while Figs. 9(b) and 10(b) show the FFT of the acting loads. In both loading cases, the highest contribution to the displacement response is at frequency zero with small peaks occurring for frequencies smaller than 0.5 Hz in Fig. 9(a).

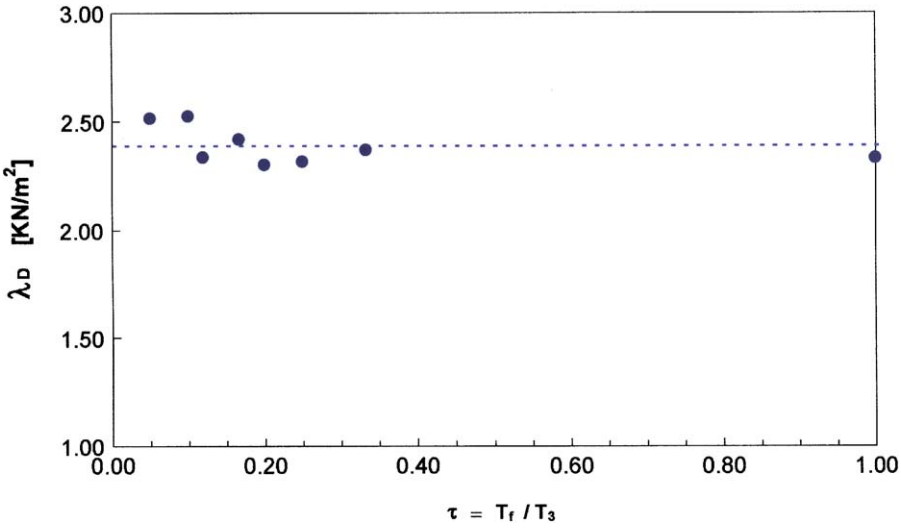

Fig. 6. Critical dynamic load λ_D for different normalized load periods $\tau = T_f/T_3$ using $\eta = 0.1$; ●, λ_{Dynamic}; – – –, λ_{Mean}.

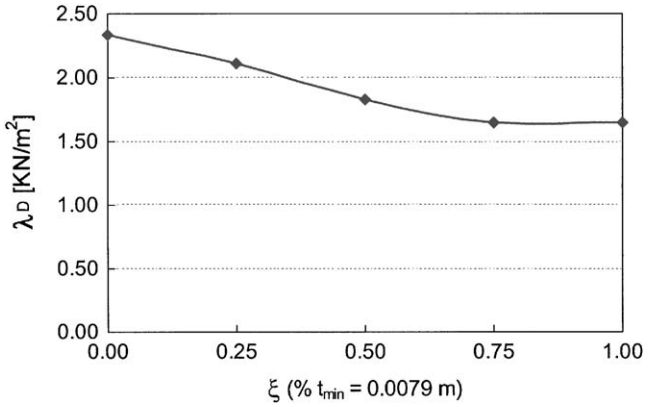

Fig. 7. Summary of analysis of sensitivity to imperfections of λ_D for $\eta = 0.1$ and $T_f = 0.3562$ seg.

The FFT of the response for constant pressure shows peaks for low frequencies that may be due to the period of the oscillations after the tank has buckled. This period is 2.78 s (frequency 0.35 Hz) and this is what can be observed for the third peak in Fig. 9(a). The FFT of the response for the fluctuating pressure is shown in Fig. 10(a). Following buckling, the period of oscillation is 0.85 s (1.43 Hz), for which the FFT shows a small peak showing a maximum value.

The possibility of coupling between the excitation (Figs. 9(b) and 10(b)) and the response (Figs. 9(a) and 10(a)) has been considered, but it seems that only for frequency zero there is a strong coupling and there are only minor effects for higher frequencies. This suggests that even for the case of fluctuating load, resonance does not occur.

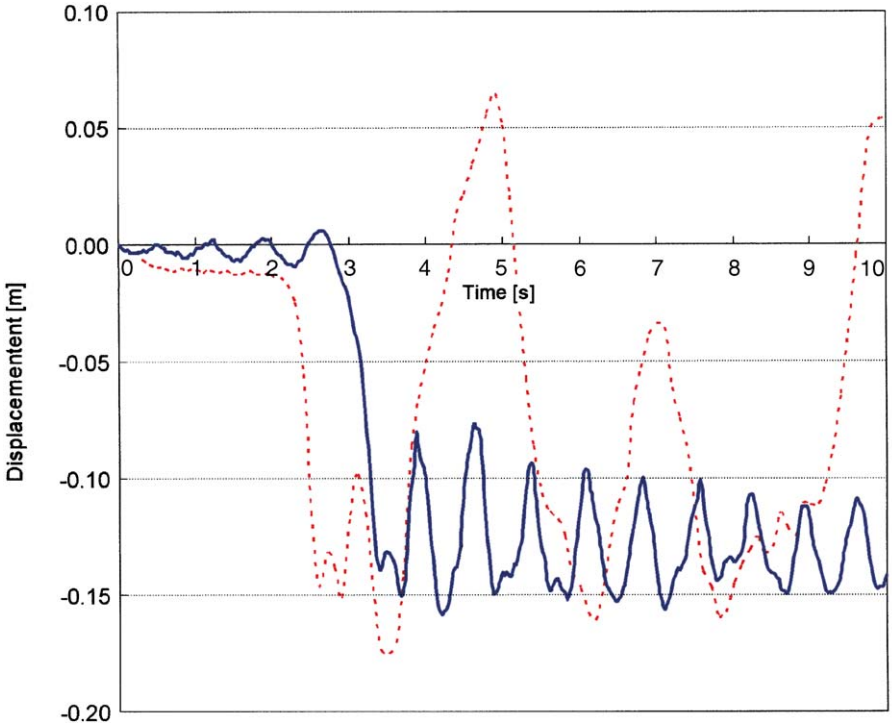

Fig. 8. Maximum response of node A recorded during 10 s for constant load: – – –, $\lambda_D = 2.515$ and fluctuating load: —, $\lambda_D = 2.34$ ($\eta = 0.1$, $T_f = 0.3562$ s).

An alternative analysis was to split the response to distinguish between the prebuckling and the postbuckling transient displacements, and to compute the FFT for each part separately. The results are drawn in Fig. 11(a) for the rectangular impulse and in Fig. 11(b) for the fluctuating load. Again, it may be seen that the maximum response is for zero frequency and that there are no peaks with large amplitude for higher frequencies.

6. Conclusions

The time domain results computed in this research indicate that for a deterministic model of velocity and pressure variations, a change in the period of oscillations does not produce a significant change in the dynamic buckling load.

For small periods of pressure fluctuations, the dynamic buckling load is close to the value obtained with a rectangular impulse of the same duration, and for periods longer than the natural period of the structure the same situation occurs. The coincidence of the period of excitation with the natural period of the tank does not induce large changes in the buckling strength.

The simpler pressure model based on a 3 s rectangular impulse yields dynamic buckling loads only 5% higher than the worst situation considering pressure fluctuations. The small changes in buckling load of short tanks due to a wide range of fluctuations seem to suggest that it would not

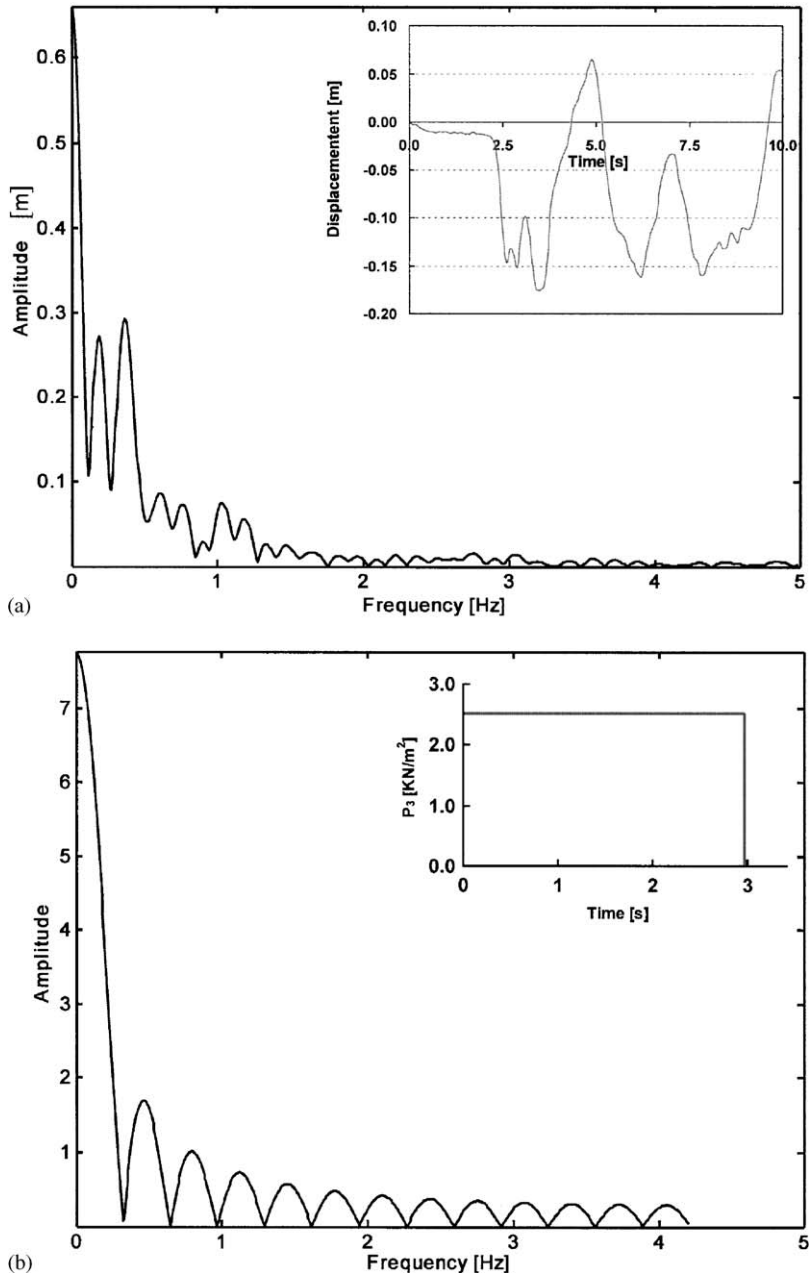

Fig. 9. FFT of (a) response to a pressure constant in time; (b) constant load function ($\lambda_D = 2.515$).

be necessary to obtain a more refined record of wind velocities to account for wind changes at intervals less than 3 s for this class of structures. The inclusion of Rayleigh damping in the model did not change the results by more than 1% with a damping ratio of 3%; however, imperfections were found to play an important role. For imperfections with the shape of the buckling mode, the

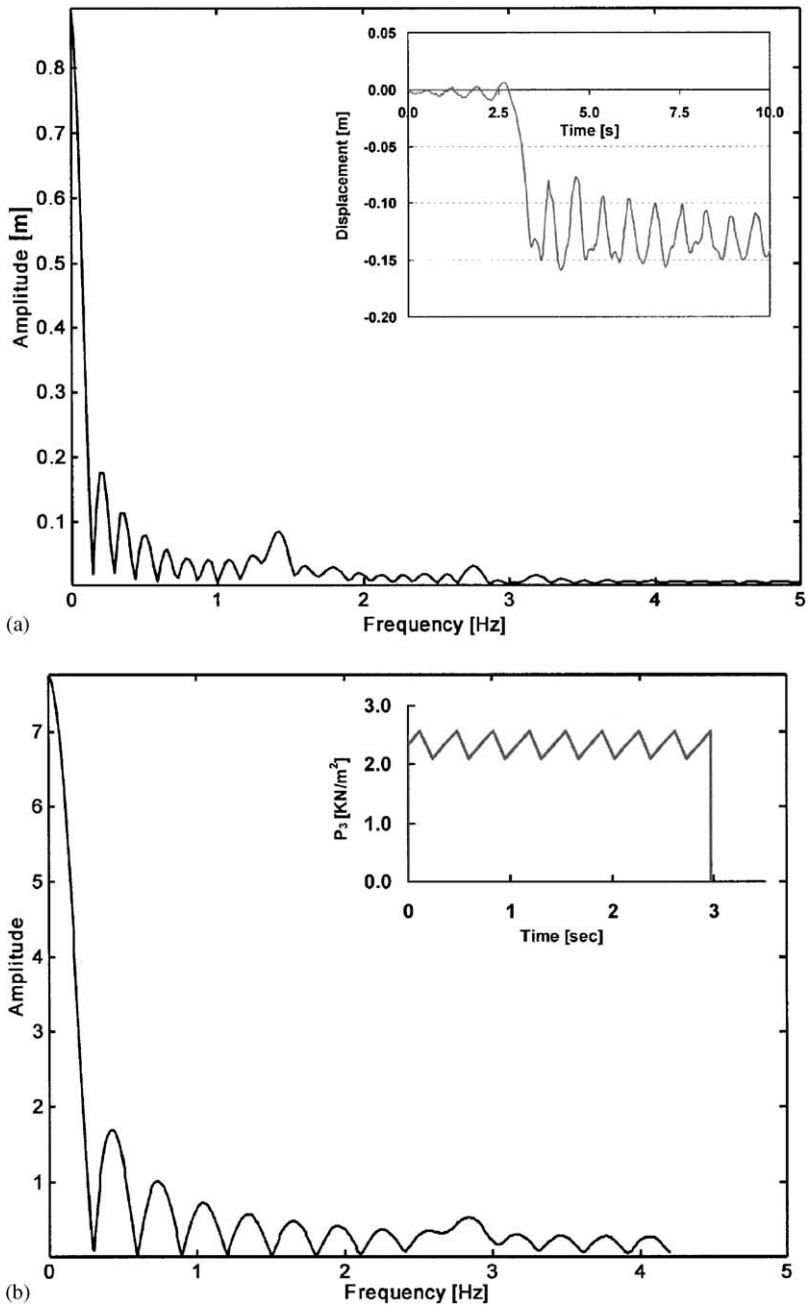

Fig. 10. FFT of (a) response to a fluctuating load; (b) fluctuating load function ($\lambda_D = 2.3\times$, $T_f = 0.356$ seg, $\eta = 0.1$).

dynamic buckling load was reduced following a pattern similar to static buckling problems, with reductions of 30% for imperfections of the order of the thickness. This effect, however, is not due to the fluctuating load and is associated with the sensitivity of the shell itself, so that the same sensitivity is detected for tanks under pressure constant in time.

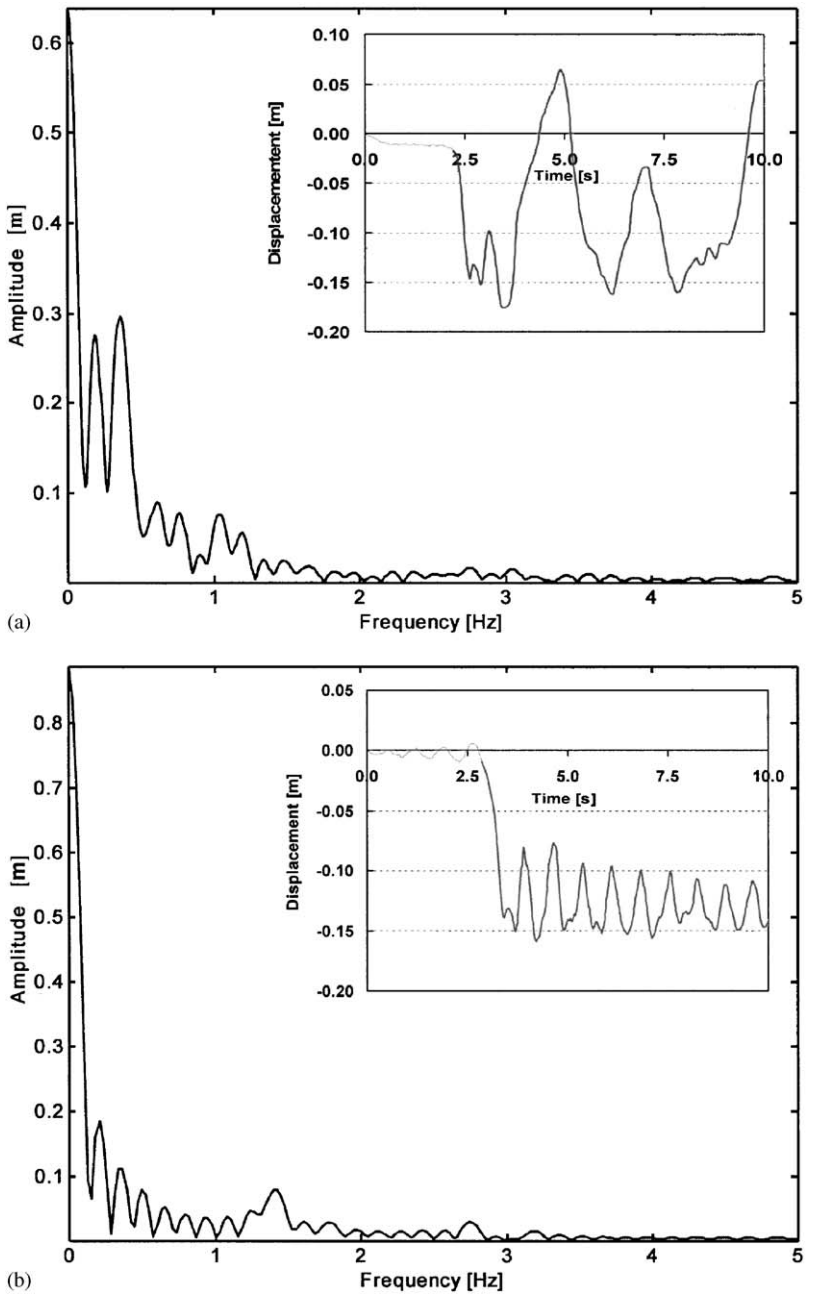

Fig. 11. FFT of the response in the buckled state considered separately: (a) constant load, high amplitude oscillations; (b) fluctuating load, high amplitude oscillations.

The results computed in the frequency domain illustrate the close similarity between the FFT of the load and the response, for both rectangular impulse and fluctuating load. In all cases, the peaks in the FFT of load and response occur for frequency zero. For higher frequencies, within

the range of the lowest natural frequencies of the tank, the peaks have small amplitudes so that resonance may be ruled out as a likely effect.

The results discussed previously indicate that dynamic effects do not dominate the response for short tanks, so that static buckling models may provide a reasonable approximation to the buckling strength of the shell under deterministic wind simulations.

Acknowledgements

This work was supported by NSF grant CMS-9907440, and by FEMA grant PR-0060-A. Their contribution is gratefully acknowledged. The authors thank the valuable comments and suggestions received from Prof. Luis E. Suarez, from Prof. Carlos A. Prato, and from two anonymous reviewers.

References

[1] P. Myers, *Aboveground Storage Tanks*, McGraw-Hill, New York, 1997.
[2] F.G. Flores, L.A. Godoy, Buckling of short tanks due to hurricanes, *Engineering Structures* 20 (8) (1998) 752–760.
[3] F.G. Flores, L.A. Godoy, Forced vibration of silos loading to buckling, *Journal of Sound and Vibration* 224 (3) (1999) 431–454.
[4] L.A. Godoy, F.G. Flores, Imperfection sensitivity to elastic buckling of wind loaded open cylindrical tanks, *Structural Engineering and Mechanics* 13 (5) (2002) 533–542.
[5] American Society of Civil Engineers, *ASCE-7-02: Minimum Design Loads for Buildings and other Structures*, ASCE, New York, 2000.
[6] M.A. Martínez, L. García, M. Doblaré, Estudio de la aparición de fenómenos de inestabilidad en silos metálicos frente a presiones del grano y acciones del viento, *Revista International de Métodos Numéricos para Cálculo y Diseño en Ingeniería* 17 (2) (2000) 199–218.
[7] R. Greiner, Cylindrical shells: wind loading, in: *Silos*, EFN Spon, London, 1998, pp. 378–399 (Chapter 17).
[8] R. Greiner, P. Derler, Effect of imperfections on wind loaded cylindrical shells, *Thin-Walled Structures* 23 (1–4) (1995) 271–281.
[9] S. Jerath, H. Sadid, Buckling of orthotropic cylinders due to wind load, *Journal of Engineering Mechanics* 111 (5) (1985) 610–622.
[10] P.S. Kundurpi, S. Gopalacharyulu, D.J. Johns, Stability of cantilever shells under wind loads, *Journal of Engineering Mechanics* 101 (EM5) (1975) 517–530.
[11] S. Gopalacharyulu, D.J. Johns, Cantilever cylindrical shells under assumed wind pressures, *Journal of the Engineering Mechanics Division* 99 (EM5) (1973) 943–956.
[12] P.A. Macdonald, K.C.S. Kwok, J.D. Holmes, Wind loads on circular storage bins and tanks: I. Point pressure measurements on isolated structures, *Journal of Wind Engineering and Industrial Aerodynamics* 31 (1988) 165–188.
[13] L.A. Godoy, E.M. Sosa, Localized support settlements of thin-walled storage tanks, *Thin-Walled Structures* 41 (2003) 941–955.
[14] H.D. Hibbitt, B.I. Karlsson, P. Sorensen, *ABAQUS, Version 6.3, Theory and User's Manuals*, Hibbitt, Karlsson and Sorensen Inc., Rhode Island, 2003.
[15] B. Budiansky, S. Roth, Axisymetric dynamic buckling of clamped shallow spherical shells, NASA Collected Papers on Stability of Shell Structures TN-1510, 1962, pp. 597–606.